Hindawi
Journal of Chemistry
Volume 2022, Article ID 8254447, 7 pages
https://doi.org/10.1155/2022/8254447

Research Article

Preparation of Ultrafine Disperse Dyes Based on the Efficiency Balance of Grinding and Dyeing

Jingsi Qiu[1] and Yue Liu[1,2]

[1]*School of Textile and Apparel, Shaoxing University, Shaoxing, Zhejiang 312000, China*
[2]*Key Laboratory of Clean Dyeing and Finishing Technology of Zhejiang Province, Shaoxing, Zhejiang 312000, China*

Correspondence should be addressed to Yue Liu; liuyue846@163.com

Received 25 July 2022; Revised 4 November 2022; Accepted 7 November 2022; Published 18 November 2022

Academic Editor: Ashanul Haque

As dispersive dyes are nonionic dyes, the particle size and particle-size distribution will significantly affect the dyeing performance. In this study, the grinding conditions, the granularity of disperse dye, and the dyeing performance were combined to study their connection further and to get better grinding process parameters for monoazo-structure disperse dyes. Through experimental research on three factors, namely, grinding time, size of grinding media, and mass ratio of grinding media to dyes, the preferred results are as follows, which could be selected based on different grinding purposes in detail. The grinding media group is Φ1 mm/Φ0.1 mm (1 : 1 mass ratio) or Φ3 mm/Φ1 mm (1 : 1 mass ratio), the mass ratio of grinding media to dyes is 5 : 1 or 10 : 1, and the grinding time range is 2–5 h. These parameters can make the overall work of coarse dyes' grinding and dyeing more efficient, avoiding the waste of cost and the increase in workload.

1. Introduction

With the continuous optimization and development of differential production technology and products' wearability in the polyester industry, this kind of fiber product has occupied the first position in textile materials for many years. According to the reports [1, 2], polyester's world filament yarn output in 2019 had grown to 46 million tons with an overwhelming industry share of more than 80%, and polyester also had a growth in 2020 though the pandemic pummeled the textile-related industry. This information lets us know that the dominant position of polyester in the industry will stay the same for a long time. At the same time, the corresponding disperse dyes for dyeing and printing polyester textiles are increasingly abundant in quantity and variety and better in quality.

The dyeing performance of polyester textiles is limited by various constituent factors of disperse dyes, such as structural type [3], particle size [4], crystal structure [5], blending ratio, dispersant type [6, 7], and others. Currently, the research on disperse dyes for textiles mainly focuses on their synthesis. The dyes have better dyeing performance by changing their structure type. For example, the disperse dye with two urethane groups in the molecule has great colorfastness to washing and sublimation [8]. Of course, changing the structure can also make the disperse dyes functional, such as disperse dyes with a coupling component of a novel cyanoacetyl microcrystalline cellulose derivative [9]. Its dyed or printed fabrics have high antibacterial effects and colorfastness. In addition, since 1922, some researchers have studied ceaselessly temporarily solubilized disperse dyes with water-soluble groups that differed from conventional disperse dyes [10–12]. As a result, they are dispersant-free in use and predictably beneficial to the environment. Because of that, it is necessary to add dispersants to avoid agglomeration in disperse dyes' effective use. The powder's granularity of commercial disperse dyes is mostly at the micron scale. Changes in technological factors such as temperature during dyeing could cause dyes to agglomerate or recrystallize and lead to some defects such as color spots or colorfastness reduction of dyed textiles in the end. Hence, in the daily study and use of disperse dyes, we all have a

consensus that commercial disperse dyes generally contain about 30–60% dispersants. Of course, some dispersants' performance may also be reduced at high-temperature dyeing. These dispersants, which are nonabsorbable by fibers, impose a heavy burden on wastewater treatment and environmental protection. Some dispersants that can improve the dispersibility and stability of disperse dye suspensions have been researched and developed to enhance efficiency [13], and this will be a hope to reduce the dosage of dispersants.

Excluding the factors of dye structure and dispersants was studied a lot and has been mentioned previously, and this paper focuses on the particle sizes and their distribution of dyes. One of the critical industrial production processes of water-insoluble disperse dyes is grinding after adding dispersants, which cannot be changed in a short time. The grinding process needs attention as the particles' sizes and distribution will directly affect the dyeing properties [14]. In the study of ultrasound effects on the sizes of disperse dyes, there is a conclusion that granularity reduces with the ultrasonic action, and therefore, the diffusion and adsorption of dye in fibers increase [15]. The relationship between partial grinding process conditions, such as dispersant and grinding speed, and the particle sizes of the dye had been described in another recent study [16]; it lets us know that the higher grinding conditions are set, such as longer time and faster rotation rate of grinding, the smaller particle sizes can be obtained. However, there is a real problem: what grinding conditions can improve the efficiency of the whole work, from grinding to dyeing or printing, in our research or production.

In our work, we combined the grinding conditions, the granularity of disperse dyes, and the dyeing performance to study their connection further and to get efficient grinding process parameters for monoazo-structure disperse dyes when the dyeing performance is close or better. We changed the grinding time, the diameters of the grinding media, the mass ratio of grinding media to dyes, and the structure types of dyes. The dispersant in the experimental dye and the pH of the dye solution were the same, and no salts were used. In addition, the sizes of disperse dye particles under different grinding conditions were investigated by using a planetary ball mill and a laser particle size analyzer. Spectrophotometers also measured the dyeing K/S values of disperse dyes with characteristic particle sizes.

2. Experiment

2.1. Materials. The commercial disperse dyes and industrial dye filter cake, C. I. Disperse Yellow 42 (Y42) and C. I. Disperse Orange 31 (O31), were both from Hangzhou Flariant Co., Ltd, China. Dispersant MF and soap powder were of industrial grade from Hangzhou Flariant Co., Ltd, China. PET fabrics (Zhejiang RGB Textile Printing and Dyeing Co., Ltd, China). The following purchased chemicals are both analytical reagents: absolute ethanol (Shanghai Fuming Chemical Reagent Factory, China), sodium hyposulfite (Jiangsu Qiangsheng functional Chemistry Co., Ltd, China), acetic acid (Zhejiang Yida Chemical Reagent Co., Ltd, China), sodium hydroxide (Guangdong Xilong Chemical Plant Co., Ltd, China), and sodium carbonate (Hangzhou Dafang Chemical Reagent Co., Ltd, China).

2.2. Grinding of Disperse Dyes. Dyes and chemicals were weighed by using MS204S electronic balance (Mettler Toledo Instruments Co. Ltd., Switzerland). Two different structures of disperse dyes were selected, Y42 (molecular weight 369.41) with nitrodiphenylamine structure and O31 (molecular weight 381.38) with monoazo structure; their specific structures are shown in Figure 1. Each dye filter cake was uniformly mixed with the dispersant MF (sodium methylene dimethyl naphthalene sulfonate) at a mass ratio of 6 : 4 as the experimental dye and the commercial dyes as the original sample without regrinding. Then, wet grinding of experimental dyes was carried out. The dyes were ground by using the Retsch PM400 floor-type planetary ball mill (Retsch GmbH, China Headquarter), and the grinding media were zirconia beads with different diameters.

2.2.1. Change the Diameters of Grinding Media. The experimental dyes (10 g) of O31, grinding media, deionized water (20 ml), and absolute ethanol (5 ml) were added to the ball mill and subsequently ground for 7 hours at 500 r/min.

The diameters (symbol Φ, unit mm) of grinding media were as follows: 6, 3, 1, 6/1 (1 : 1), 3/1 (1 : 1), 3/1 (7 : 3), and 1/0.1 (1 : 1), the specific numbers in brackets represent the mass ratios of different diameters media. The recipes of the material mixture were devised into seven groups according to these media, and the mass ratio of grinding media to dyes was 2 : 1 in each group.

2.2.2. Change of Grinding Time. The experimental dyes (10 g) of O31, grinding media (Φ1 mm, 5 g), deionized water (20 ml), and absolute ethanol (5 ml) were added to the ball mill. This recipe was copied for five groups, and the grinding time was set as 2 h, 5 h, 7 h, 9 h, and 11 h, respectively. Similarly, the rotational speed was 500 r/min.

2.2.3. Different Mass Ratios of Grinding Media to Dyes. The experimental dyes (10 g) of O31, grinding media (Φ1 mm), deionized water (20 ml), and absolute ethanol (5 ml) were added to the ball mill and subsequently ground for 7 hours at 500 r/min. The mass ratio of grinding media to dyes was 1 : 1, 5 : 1, 10 : 1, and 20 : 1, respectively.

2.2.4. Different Structure Types of Disperse Dyes. The experimental dyes (10 g) of Y42, grinding media (Φ1 mm, 5 g), deionized water (20 ml), and absolute ethanol (5 ml) were added to the ball mill. The grinding time was set as 5 h and 8 h. The rotational speed was 500 r/min.

2.3. Dyeing PET Fabric. Different particle sizes of O31 obtained by the above grinding experiments were used for dyeing polyester fabrics and compared with the dyed fabrics with commercial disperse dyes. Fabrics were dyed by using

Datacolor Ahiba IR low liquor ratio dyeing machine (Datacolor Co., USA), and the dyeing process referred to Reference [7]. The concentration of the dyes in the dyeing solution was 2% (OWF). The fabric samples were moistened and squeezed, then dyed in a dye bath consisting of the dyeing liquor and acetic acid (adjusted pH value of 4.5–5.5) with liquor ratio (L. R) 1 : 30. Fabrics were immersed at room temperature, and the temperature was increased to 130°C at a rate of 2°C/min. Then, the dyeing process was maintained for a predetermined soaking time at 130°C, and the time (unit min) was set as follows: 3, 5, 10, 15, 30, and 45. Next, the fabrics were washed with hot water after the temperature was reduced to 80°C at a rate of 3°C/min. Then, the reduction-clearing process was carried out in a solution containing sodium hyposulfite (3 g/L) and sodium hydroxide (2 g/L) with L. R 1 : 30 for 5 minutes at 80°C. These treated samples were rinsed with hot water before soaping. The soaping process was implemented in a solution consisting of sodium carbonate (2 g/L) and soap powder (5 g/L) for 10 minutes with L. R 1 : 30 at 95°C. Then, the fabrics were rinsed and dried with a UF260Plus universal forced convection oven (Memmert GmbH, Germany) at 80°C.

2.4. Characterization

2.4.1. Disperse Dye Particle Size Measurements. The disperse dye solutions were ultrasonically homogenized, and then these dye particles' sizes and their distribution were measured by using the Mastersizer 3000 (Malvern Instruments Ltd, UK) laser particle size analyzer.

2.4.2. Color Yield Measurements. The color yield (K/S) values of the dyed fabrics were determined by using Datacolor 600 spectrophotometers (Datacolor Co., USA) using artificial daylight 6500 K at 10° observer. Five different positions on the same dyed fabric were selected for testing. The K/S values of the dyed cloth were selected at 465 nm, which is the maximum absorption wavelength of O31.

3. Results and Discussion

3.1. Effect of Grinding Media Diameters. The mass ratio of grinding media to dyes was set as 2 : 1, and the grinding media diameters and their mass ratios were adjusted. The granularity of the dyes after 7 hours of wet milling is shown in Table 1, and Figure 2 shows the particle size distributions of the original sample and after grinding with Φ1 mm, Φ3 mm, and Φ6 mm media.

Compared with the curves in Figure 2, the original sample particles of commercial O31 were mostly distributed around 1 μm. After the grinding of the filter cake, the distribution curve was inclined in the direction of small size, which indicated that the dyes were effectively crushed due to the action of grinding media and dispersant. A general trend could also be seen from the data in Table 1 that the proportion of dyes with small granularity increased markedly with the decrease in the diameter of the grinding media. However, there were unsatisfactory phenomena of double-peak and curve tailing. In the literature, these were caused by some experimental operations, which led to the secondary aggregation and size increase of particles. One of the reasons was that the concentration of the test sample was not diluted enough, and another was the simultaneous use of chemical dispersion (e.g., surfactant) and physical dispersion (e.g., ultrasound) [17, 18]. According to Table 1, at least 50% of the dye particle sizes were lower than 75.3 nm when dyes were ground with Φ3 mm media. Also, some values in this table show that the mass ratio of media with different diameters similarly had an unusual effect on reducing the dye particle sizes.

From the grinding mechanism of the planetary ball mill [19], the grinding effect and efficiency depend on the times of collisions between dyes and grinding media within a certain volume and time. To maximize collision efficiency, the grinding process requires that media have enough momenta or mass to generate stress making the dye crystals fracture. So obviously, successful grinding cannot be performed if the media are too small. On the other hand, if the grinding media are too large, although there are sufficient momentums to make the dyes collide with the media and grinding tank frequently and availably, the large volume gap and the small contact area between the media and dyes will lead to local agglomeration of the dyes and increase the particle diameters. Large and small grinding media also collide with each other when they are mixed, and this consumes energy and reduces the chance of crashes between media and dyes. Hence, from the perspective of dye particle sizes and distribution, there are some suitable diameters and ratios of grinding media. In addition, from the perspective of the Dv (90) data which was less than perfect, this meant that when the volume distribution reached 90%, there were a few large dye particles with a diameter of tens or even hundreds of microns. In other words, there was a part with a very inhomogeneous distribution of the dye's granularity despite the conditions of different grinding media. The agglomeration of some dyes and the antigrowth phenomenon of particle diameters were triggered by the abovementioned reasons of curve tailing, double-peak, and insufficient grinding caused by the small mass ratio of grinding media to dyes. In this experiment, it was apparent that using the grinding media group of "Φ3 mm/Φ1 mm (1 : 1 mass ratio)" or "Φ1 mm/Φ0.1 mm (1 : 1 mass ratio)" could make O31 obtain a better-grinding result. When we consider the difficulty of filtering the media after grinding, choosing the former media group can make the operation easier if the requirements for the dye particle size are not particularly high.

3.2. Effect of Grinding Time. O31 was ground for different times of 2–11 hours. The dye particle size data and their distributions are shown in Table 2 and Figure 3.

As seen from the data in Table 2 and the corresponding distribution diagrams, the distribution curves of dye particle sizes gradually moved to the left with the extension of grinding time, and values at 50% volume density inclined to cut down. The volume densities of dyes with particle sizes

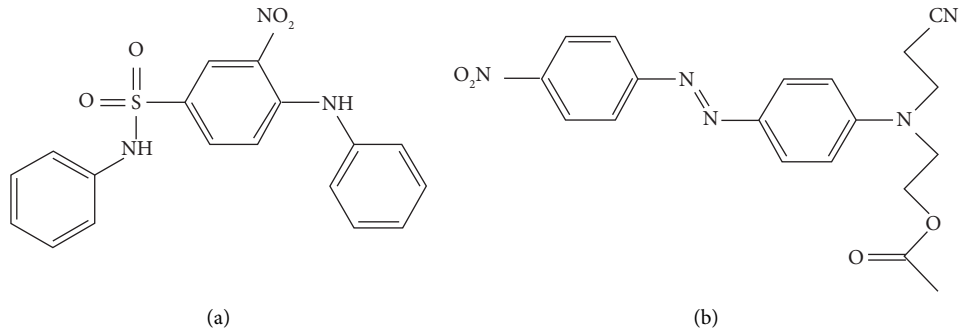

Figure 1: The structures of different dyes used in the experiment (a) Disperse yellow 42, (b) Disperse orange 31.

Table 1: Particle sizes of dispersed orange 31 with different media diameters and mass ratios.

	Original sample	Grinding media diameters (mm) and mass ratios (numbers in brackets)						
		6	3	1	6/1 (1 : 1)	3/1 (1 : 1)	3/1 (7 : 3)	1/0.1 (1 : 1)
<100 nm (%)	2.33	47.72	57.74	54.72	44.21	59.70	57.00	60.26
<200 nm (%)	23.82	51.87	62.46	59.33	48.15	67.17	62.37	65.36
Dv (10) (nm)	168.00	21.50	19.70	20.20	22.30	20.00	20.10	19.50
Dv (50) (nm)	401.00	143.00	75.30	85.40	671.00	73.90	78.80	70.00
Dv (90) (μm)	1.48	227.00	153.00	275.00	1020.00	43.40	72.70	16.90

a. The percentage is based on volume. b. Dv (10), Dv (50), Dv (90): 10%, 50%, and 90% of the volume distribution, and their numbers represent the measured sizes when the cumulative volume distribution percentage reaches 10%, 50%, and 90%, respectively.

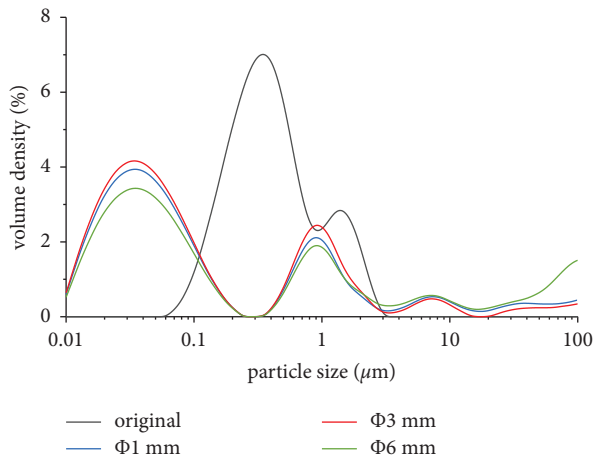

Figure 2: Particle sizes' distribution of original dispersed orange 31 samples and after grinding with Φ1 mm, Φ3 mm, and Φ6 mm media.

less than 100 nm increased significantly within 2–5 h of grinding time, and then the growth of content with small particles slowed down or tended to fall when the time continued to extend to 7 to 11 h. This showed that as the grinding time increases and the small sizes of dyes reach a certain amount, the dispersion and agglomeration of dyes will be balanced. So, the decreasing dye granularity would be unnoticeable, and the grinding efficiency would be reduced if the grinding time was too prolonged. In brief, the better grinding time of the disperse dyes in this experiment was around 5 h.

Table 2: Particle sizes of dispersed orange 31 with different grinding times.

	Original sample	Grinding time (h)				
		2	5	7	9	11
<100 nm (%)	2.33	7.72	60.88	54.72	59.23	39.83
<200 nm (%)	23.82	40.62	66.81	59.33	65.39	61.00
Dv (10) (nm)	168.00	123.00	19.50	20.20	19.90	31.20
Dv (50) (nm)	401.00	286.00	69.20	85.40	73.70	162.00
Dv (90) (μm)	1.48	0.68	4.59	275.00	25.20	1.34

3.3. Effect of Mass Ratios of Grinding Media to Dyes. The experimental data are shown in Table 3. It could be seen that with the increased weight of grinding media, the reduction range of granularity and the content of small particle-size dyes increased signally. For example, when the mass ratio of the grinding media to the dye was 10 : 1, particle diameters of the 50% dyes were less than 78.7 nm which was also smaller than the value at the mass ratio of 1 : 1 to 5 : 1. With the rising proportion of media, the effective friction and collision between media and dyes during grinding also increased easily. Then, the dye particle sizes could be reduced greatly. However, it would cause partial aggregation of dyes if the number of media was excessive. For example, when the mass ratio of dye to the medium was 1 : 20, the values of Dv (50) were small, but the granularity of some dyes had grown to tens of microns. These data made clear that O31 could get a much smaller particle size when the mass ratio of media to dyes was 5 : 1 or 10 : 1. Of course, choosing the former could reduce the workload of media filtration if the large particle problem is not cared about.

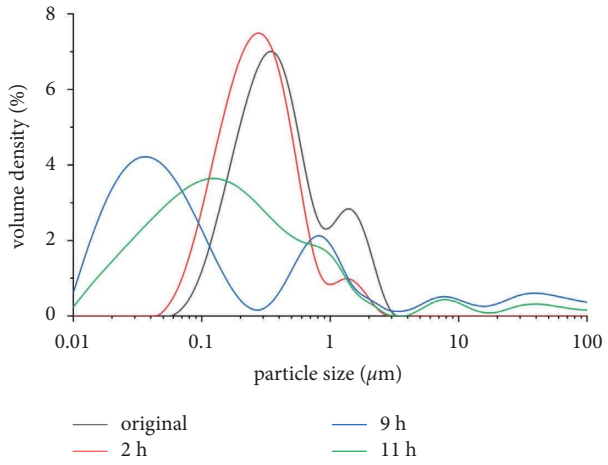

Figure 3: Dispersed orange 31 particle sizes' distribution after grinding for 2 h, 9 h, and 11 h.

Table 3: Particle sizes of dispersed orange 31 with different mass ratios of grinding media to dyes.

	Original sample	Mass ratios of grinding media to dyes			
		1 : 1	5 : 1	10 : 1	20 : 1
<100 nm (%)	2.33	33.76	48.61	60.08	60.69
<200 nm (%)	23.82	57.17	74.74	73.05	67.31
Dv (10) (nm)	168.00	41.70	32.00	21.30	19.80
Dv (50) (nm)	401.00	191.00	117.00	78.70	70.70
Dv (90) (μm)	1.48	2.58	0.76	1.81	37.60

3.4. Effect of Dyes with Different Types of Structures. Y42 was ground for hours, and the results are shown in Table 4. The particle size distribution after grinding for 8 h is displayed in Figure 4.

From the data comparison, there was no big difference between the original particle sizes (commercial dyes) of O31 and Y42. The result showed that the distribution of O31 shifts significantly toward the small particle-size direction after 5 hours of grinding. The volume densities of O31 with granularity less than 100 nm and 200 nm had reached 60.88% and 66.81%, respectively. Under the same conditions, the volume densities of Y42 were only 0.63% and 24.19%, respectively. Looking at Figure 4, the curves of Y42 showed that particle sizes changed a little compared with those of the original sample after grinding for 8 h. All of these illustrated the fact that the dye crystals of Y42 with nitrodiphenylamine structure, which has three benzene rings and greater intermolecular forces, were less susceptible to breaking and refining than that of O31 with monoazo structure. Therefore, distinct grinding processes were required for disperse dyes with diverse types of structures.

3.5. Dyeing Properties of Disperse Orange 31 with Different Particle Sizes. The dyeing depth was used here to illustrate the dyeing properties of the dye. Table 5 showed the test

Table 4: Particle sizes of dyes with different types of structures under the same grinding process.

	O31		Y42		
	Original	5 h	Original	5 h	8 h
<100 nm (%)	2.33	60.88	0.00	0.63	2.64
<200 nm (%)	23.82	66.81	9.67	24.19	33.36
Dv (10) (nm)	168.00	19.50	245.00	182.00	153.00
Dv (50) (nm)	401.00	69.20	466.00	348.00	308.00
Dv (90) (μm)	1.48	4.59	1.15	0.64	0.58

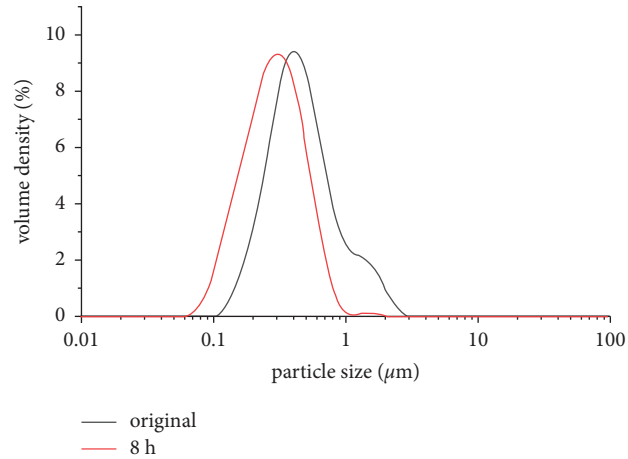

Figure 4: Particle size distributions of the original disperse yellow 42 sample after grinding for 8 h.

results of dyed PET fabrics' *K*/*S* values with the conditions of 2% (OWF) dye concentration, various particle sizes of O31, and different dyeing times. These dyes with specific particle sizes characterized by using Dv (50) were selected from the above experiments. The selected experimental dyes could be regarded in 4 size ranges: <100 nm, <200 nm, <300 nm, and <700 nm.

In the printing and dyeing industry, it is well known that reducing the sizes of disperse dye particles will not only shorten the dyeing time but also obtain higher dye uptake, which also can be seen in Table 5. The *K*/*S* values of fabric examples at the same dyeing time elevated continuously with the decrease of dye granularity. Conspicuously, the *K*/*S* values of nanoscale, 70 nm characterized by using Dv (50), were higher than that of other particle sizes. But with the extension of dyeing time, the difference in *K*/*S* values of dyed fabrics with the same particle-size dyes tended to lessen. Overall, the apparent color yield *K*/*S* values of these dyes were about 25, which could be considered the basic dynamic equilibrium of dyeing. The dyeing equilibrium time for the dye with a particle size of about 286 nm was 45 minutes, the same as that of 401 nm (the original dye). However, the dyeing *K*/*S* values of 70 nm and 162 nm dyes at 15 min were already pretty close to their respective values at 45 min. Therefore, it gave evidence that the dyes of these two sizes had reached the dyeing equilibrium within 15 minutes. Compared with the final *K*/*S* value of the original dye (the commercial O31), we could get a result that a better

Table 5: *K*/*S* values of dyed fabrics with disperse orange 31 at different particle sizes and dyeing times.

Dyeing time (min)	*K*/*S* values				
	671 nm	401 nm (original)	286 nm	162 nm	70 nm
3	14.99	15.45	16.49	17.50	18.77
5	17.80	17.97	18.08	19.73	20.92
10	20.97	21.16	22.35	23.35	23.80
15	23.01	24.08	24.32	24.94	25.80
30	23.99	24.11	24.41	25.04	25.90
45	24.32	24.96	25.17	25.23	25.93

efficiency balance between the overall work of grinding and dyeing could be achieved by choosing a grinding process that could make the Dv (50) particle size 100–300 nm. If you focus on improving the dyeing properties of disperse dyes, choose the grinding process that can make the Dv (50) particle size in the range of less than 100 nm; that is, choose the preparation process of nanoscale dyes.

4. Conclusion

The smaller the particle size of the disperse dye, the shorter time for the dye to reach dyeing equilibrium, and the higher dye uptake the fabric can obtain. Therefore, particle size and its distribution of disperse dye are one of the focal points to optimize dyeing performance, while grinding condition is an important factor affecting the particle size and its distribution. Based on these, this paper focuses on the grinding process to obtain grinding parameters with a better balance between grinding inputs and dyeing outputs to make the work more efficient.

Taking the filter cake and its commercial dye of Dispersed Orange 31 as an example, better parameters were obtained by comparing the experimental results of three factors, namely, grinding time, the sizes of grinding media, and the mass ratio of grinding media to dyes. The preferred results are as follows: the grinding media group is Φ1 mm/Φ0.1 mm (1 : 1 mass ratio) or Φ3 mm/Φ1 mm (1 : 1 mass ratio), the mass ratio of grinding media to dyes is 5 : 1 or 10 : 1, and the grinding time is 2–5 h. These can be selected based on different grinding purposes, such as grinding simply to achieve the same dyeing effect as commercial dyes, improving dye uptake, reducing dyeing time, and so on.

In addition, we have proved from the experiment that the better grinding process is varied for different structure types of disperse dye. For example, Disperse Yellow 42 with nitrodiphenylamine structure had greater intermolecular forces than Disperse Orange 31 with monoazo structure, which was why the former was more difficult to grind well. Therefore, the results of this study provide an appropriate and valuable reference for the grinding process of monoazo disperse dyes with similar structures. The dyeing performance of disperse dyes is also affected by other factors, such as salts, type of dispersant, and pH; these parts need further study and discussion.

Data Availability

The datasets used or analyzed during the current study are available from the corresponding author upon reasonable request.

Conflicts of Interest

The authors declare that they have no conflicts of interest.

Acknowledgments

The authors are sincerely thankful for the equipment support and technical assistance provided by the Key Laboratory of Clean Dyeing and Finishing Technology of Zhejiang Province, China.

References

[1] A. W. Engelhardt, "The fiber year 2021—key findings," 2021, https://fiberjournal.com/the-fiber-year-2021-key-findings/.

[2] A. W. Engelhardt, "The fiber year—global development of spun and filament yarns," 2021, https://fiberjournal.com/the-fiber-year-global-development-of-spun-and-filament-yarns/.

[3] M. Li, Q. X. Lu, A. P. Liu et al., "Benzyl-containing azobenzene-based disperse dyes: relationship between molecular packing and alkali-resistant stability," *Journal of Molecular Liquids*, vol. 317, Article ID 114270, 2020.

[4] T. Kim, B. Seo, G. Park, and Y. W. Lee, "Effects of dye particle size and dissolution rate on the overall dye uptake in supercritical dyeing process," *The Journal of Supercritical Fluids*, vol. 151, pp. 1–7, 2019.

[5] J. Linag, Y. Zhong, Z. P. Mao, H. Xu, L. P. Zhang, and X. F. Sui, "Effect of crystal form on dyeing behavior of disperse dyes," *Journal of Textile Research*, vol. 39, no. 7, pp. 69–73, 2018.

[6] Y. L. Qin, M. J. Yuan, Y. B. Hu et al., "Preparation and interaction mechanism of nano disperse dye using hydroxypropyl sulfonated lignin," *International Journal of Biological Macromolecules*, vol. 152, pp. 280–287, 2020.

[7] Y. Liu, L. Cheng, K. Y. Hao, and L. X. Mo, "The effect of dispersant on the dispersibility and dyeing properties of disperse purple *B* raw dyes," *Basic Sciences Journal of Textile Universities*, vol. 32, no. 2, pp. 204–211, 2019.

[8] S. J. Fang, G. F. Feng, Y. Q. Guo, W. G. Chen, and H. F. Qian, "Synthesis and application of urethane-containing azo disperse dyes on polyamide fabrics," *Dyes and Pigments*, vol. 176, Article ID 108225, 2020.

[9] G. A. M. Nawwar, K. S. A. Zaher, E. Shaban, and N. M. A. El-Ebiary, "Utilizing semi-natural antibacterial cellulose to prepare safe azo disperse dyes and their application in textile printing," *Fibers and Polymers*, vol. 21, no. 6, pp. 1293–1299, 2020.

[10] J. J. Lee, W. J. Lee, and J. P. Kim, "Dispersant-free dyeing of polyester with temporarily solubilized azo disperse dyes from indole derivatives," *Fibers and Polymers*, vol. 4, no. 2, pp. 66–70, 2003.

[11] C. R. Meena, S. Maiti, N. Sekar, S. More, and R. V. Adivarekar, "Dispersant-free disperse dyes for polyester an eco-friendly approach," *Journal of the Textile Institute*, vol. 108, pp. 1–6, 2016.

[12] J. P. Kim, J. S. Kim, J. S. Park, S. S. Jang, and J. J. Lee, "Synthesis of temporarily solubilised azo disperse dyes containing a *β*-sulphatoethylsulphonyl group and dispersant-free dyeing of

polyethylene terephthalate fabric," *Coloration Technology*, vol. 132, no. 5, pp. 368–375, 2016.

[13] T. Qian, Y. Zhong, Z. P. Mao et al., "The comb-like modified styrene-maleic anhydride copolymer dispersant for disperse dyes," *Journal of Applied Polymer Science*, vol. 136, no. 16, Article ID 47330, 2019.

[14] M. Li, K. L. Song, K. L. Xie, and A. Q. Hou, "Dispersion of disperse yellow BROB with polymer surfactants and its dyeing property for polyester fabric," *Fibers and Polymers*, vol. 16, no. 3, pp. 614–620, 2015.

[15] S. Babaei Golshan Abadi, M. E. Yazdanshenas, R. Khajavi, A. Rashidi, and M. Varsei, "Ultrasound-assisted of poly (trimethylene terephthalate) dyeing with nano-disperse blue 79: isotherms, kinetics, and thermodynamics insights," *Journal of the Textile Institute*, vol. 112, pp. 1–10, 2020.

[16] R. F. Wang, M. Li, A. L. Tian, C. X. Wang, and S. H. Fu, "Relationship between disperse yellow 6GSL crystal form and thermal stability of its dispersions," *Journal of Textile Research*, vol. 42, no. 5, pp. 96–102, 2021.

[17] M. Ryżak and A. Bieganowski, "Methodological aspects of determining soil particle-size distribution using the laser diffraction method," *Journal of Plant Nutrition and Soil Science*, vol. 174, no. 4, pp. 624–633, 2011.

[18] A. Bieganowski, M. Ryżak, A. Sochan et al., "Laser diffractometry in the measurements of soil and sediment particle size distribution," in *Advances in Agronomy*, D. L. Sparks, Ed., Academic Press, Amsterdam, Netherlands, 2018.

[19] C. F. Burmeister and A. Kwade, "Process engineering with planetary ball mills," *Chemical Society Reviews*, vol. 42, no. 18, pp. 7660–7667, 2013.